

be noted that the  $^1\text{H}$  NMR of the acetylated PVAm provides corroborating evidence for the triad analysis of PVAm, and the configurational analysis of the latter is consistent with the configurational analysis of poly(vinyl alcohol).

Registry No. *meso*-DAP, 29745-96-8; *rac*-DAP, 29745-97-9.

## References and Notes

- (1) Murano, M.; Harwood, H. J. *Macromolecules* **1970**, *3*, 605.
- (2) St. Pierre, T.; Lewis, E. A.; Levy, G. C. In "Polymeric Amines and Ammonium Salts"; Goethals, E. T., Ed.; Pergamon Press: Oxford, 1980; pp 245-248.
- (3) Wu, T. K.; Ovenall, D. W. *Macromolecules* **1973**, *6*, 582.
- (4) Chang, C.; Muccio, D. D.; St. Pierre, T.; Chen, C. C.; Overberger, C. G. *Polym. Prepr., Am. Chem. Soc., Div. Polym. Chem.* **1985**, *26* (2), 265.
- (5) Chang, C.; Muccio, D. D.; St. Pierre, T. *Macromolecules* **1985**, *18*, 2334.
- (6) Hughes, A. R.; St. Pierre, T. In "Macromolecular Synthesis"; Mulvaney, J. E., Ed.; Wiley: New York, 1977; pp 31-37.
- (7) Dawson, D. J.; Gless, R. D.; Wingard, R. E., Jr. *J. Am. Chem. Soc.* **1976**, *98*, 5996.
- (8) Overberger, C. G.; Chen, C. C. *J. Polym. Sci., Polym. Lett. Ed.* **1985**, *23*, 345.
- (9) Bosnich, B.; Harrowfield, J. M. *J. Am. Chem. Soc.* **1972**, *94*, 3425.
- (10) Freeman, R.; Kempell, S. P.; Levitt, M. H. *J. Magn. Reson.* **1980**, *38*, 453.
- (11) Kowalewski, J.; Levy, G. C.; Johnson, L. F.; Palmer, L. J. *Magn. Reson.* **1977**, *26*, 533.
- (12) Randall, J. "Polymer Sequence Determination:  $^{13}\text{C}$  NMR Method"; Academic Press: New York, 1977; p 71.
- (13) Bovey, F. A. In "High Resolution NMR of Macromolecules"; Bower, D. J., Ed.; Academic Press: New York, 1972; p 146.
- (14) The best values were calculated by a linear regression of the log form of  $(m)^2 = 0.288$ ,  $2(mr) = 0.541$ , and  $(r)^2 = 0.171$ .
- (15) Ovenall, D. W. *Macromolecules* **1983**, *17*, 1458.
- (16) Chang, C.; Muccio, D. D.; St. Pierre, T. *Macromolecules* **1985**, *18*, 2154.

## Photochemical Cleavage of a Polymeric Solid: Details of the Ultraviolet Laser Ablation of Poly(methyl methacrylate) at 193 and 248 nm

R. Srinivasan,\* B. Braren, D. E. Seeger, and R. W. Dreyfus

IBM T. J. Watson Research Center, Yorktown Heights, New York 10598.

Received October 18, 1985

**ABSTRACT:** The products of the laser ablation of poly(methyl methacrylate) (PMMA) ( $\bar{M}_n \sim 800\,000$ ) at 193 or 248 nm range from  $\text{C}_2$  through methyl methacrylate (MMA) and a solid that is a low molecular weight ( $\bar{M}_n = 2500$ ) fraction of PMMA. While the products are the same at both wavelengths, the mix is quite different. At 193 nm, 18% of the ablated polymer is MMA, whereas at 248 nm less than 1% of the polymer appeared as MMA. A semilogarithmic plot of the mass of material removed vs. the fluence shows three distinct regions. The central portion at each wavelength (80-300  $\text{mJ}/\text{cm}^2$  at 193 nm, 600-2000  $\text{mJ}/\text{cm}^2$  at 248 nm), which corresponds to rapid etching, is identified as "ablative photodecomposition". At lower fluences, the etching efficiency falls off rapidly, indicating that there is a threshold fluence. At fluences above the range for ablative photodecomposition, the etching levels off, probably due to the secondary absorption of the incoming photons by the products. The formation of  $\text{C}_2$  as a product was monitored by laser-induced fluorescence. The velocity distribution of the product as a function of fluence was also measured. The velocity distribution approaches but does not exactly fit a Maxwell-Boltzmann equation. Average translational energies as high as 6 eV were recorded even at the fluence threshold for this product. It is suggested that ablative photodecomposition involves both a one-photon process, which produces MMA and low molecular weight polymeric fragments, and a multiphoton process, which gives rise to products such as  $\text{C}_2$  with high translational energy. At longer wavelengths, a greater temperature rise within the ablated volume may be necessary to increase the quantum yield for bond-breaking. The mass of material ablated per joule of energy absorbed in the ablated volume was remarkably similar at both wavelengths. Ablative photodecomposition is a novel method to cleave an organic solid. In contrast to alternative methods such as mechanical pressure or thermal decomposition, both of which occur in the ground electronic state of the bonds undergoing rupture, ablative photodecomposition involves the electronically excited state of the bond that is broken. It may therefore limit secondary effects of the cleavage to a highly localized region, a feature that can be of considerable interest in living systems.

## Introduction

In a series of recent articles<sup>1-5</sup> we and others showed that the action of ultraviolet laser radiation causes the breakup and spontaneous removal of material from the surface of an organic polymeric solid by a process that we have termed "ablative photodecomposition". Over an area that is defined by the light beam, the surface of the solid is etched away to a depth of 0.1-4  $\mu$  at every pulse, and the products are expelled at supersonic velocity.<sup>6,7</sup> Most of the publications have been concerned with the physical and applied aspects of the removal of material. Less attention has been paid to the microscopic nature of the bond-breaking that must be fundamental to the decomposition of the polymer before ablation can occur. In this article, we are concerned with the details of the chemical process

by which photon energy causes bonds to break and results in ablation of the products. This investigation also brings up a novel aspect of the cleavage of an organic solid by a beam of photons. It will be argued that thermal energy, which can break up a solid, and mechanical force, which can also cleave a solid, are processes in the ground electronic state of a bond whereas ablative photodecomposition causes the cleavage of a solid from an electronically excited state of the bonds. It may therefore constitute a very localized process that would result in a minimum of disruption of the structure of the solid.

## Experimental Section

**Materials.** A 650- $\mu\text{m}$ -thick commercial PMMA sheet ( $\bar{M}_n \sim 800\,000$ ) was used in all of the determinations of etch depth as a function of fluence. Scanning electron microscopy (SEM) of

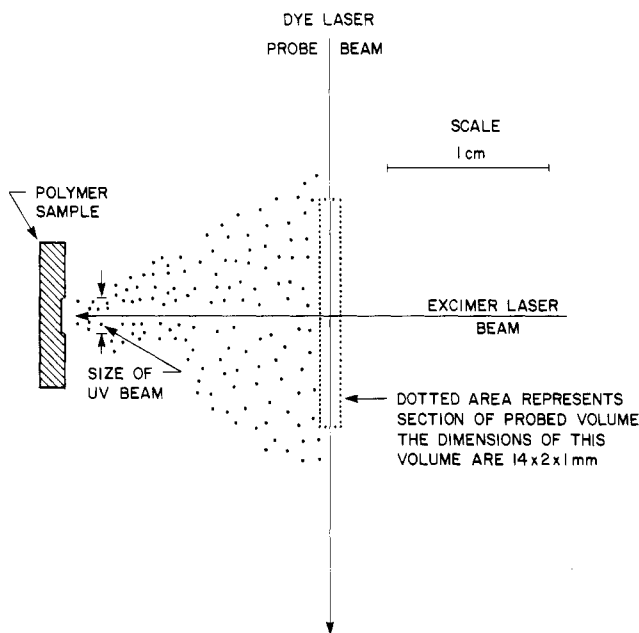


**Figure 1.** Geometry of ultraviolet laser beam and fluorescence pump beam with respect to polymer sample and fluorescence detection system (drawn to scale).

the etched area and the effluent material was also based on this sample. For the measurement of the yield of the volatile products, this sample as well as others of lower molecular weight ( $\bar{M}_n = 13\,700$ ,  $46\,400$ , or  $200\,000$ ) from Aldrich Chemical Co. were used. The latter were dissolved in acetone and spin-coated on quartz disks in order to form a film.

**Light Source.** The source of UV laser radiation was a Lambda-Physik Model 201 E excimer laser. The appropriate filling of argon and fluorine (193 nm) or krypton and fluorine (248 nm) with helium as buffer gas was used for the two wavelengths. The repetition rate of the pulses ( $\sim 15$  ns FWHM) was kept at 10 Hz or less in order to avoid any cumulative heating effect from a rapid succession of pulses. There is some evidence that with PMMA at 248 nm there is an effect of repetition rate on the etch depth per pulse at even  $\sim 3$  Hz. Therefore, at this wavelength data were taken only at 1 or 3 Hz. Experiments in which the volatile products were collected and analyzed were carried out at 0.3 Hz in order to avoid secondary photolysis of the products before they condensed in the cold trap. The fluence at the irradiated surface was measured with a Gen-Tec Joulemeter.

**Procedure.** The central uniform portion of the laser output was defined by a slit and concentrated by the use of a spherical quartz lens. The beam was further defined by a  $0.1 \times 0.3$  cm aperture that was in contact with the polymer surface. At a given fluence, a number of exposures were made at varying numbers of pulses. The etch depth of each hole was measured with a Tencor Alpha Step profilometer. The plot of etch depth vs. number of pulses (at constant fluence) was found to be linear and the line passed through the origin.<sup>8</sup> An average value of the etch depth per pulse at that fluence was obtained from the slope of the plot. All irradiations were performed in an air atmosphere at ambient room temperature. It has been shown elsewhere that the atmosphere had no measurable influence on the process of etching by UV laser radiation.<sup>9</sup>

To collect the volatile products from the laser ablation of PMMA, exposures were made on a polymer sample that was enclosed in a glass vacuum chamber fitted with a Suprasil quartz window. The chamber was pumped by a mechanical vacuum pump with two traps cooled in liquid nitrogen separating the chamber from the pump. The dynamic pressure in the chamber was 20 mtorr. The laser was pulsed at 0.3 Hz. The condensable products collected in the first trap. The second trap prevented the back diffusion of the oil vapors from the pump. The collected products were analyzed on a Hewlett-Packard Model 5995A gas chromatograph-mass spectrometer with a 3% OV-101 column 2 m long. Yields of methyl methacrylate (MMA), the only medium molecular weight product that was detected, were determined by

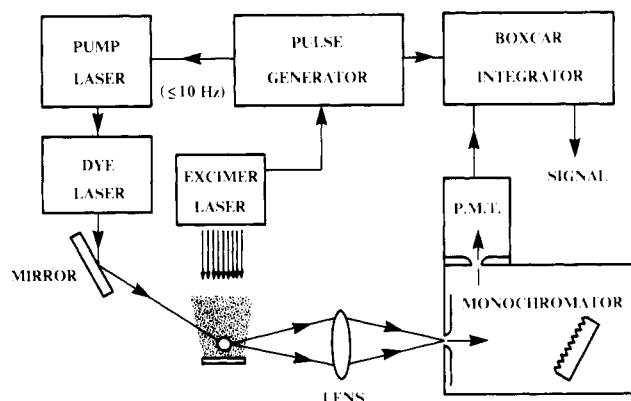


**Figure 2.** Electronic circuit for triggering ultraviolet and fluorescence pump pulses and monitoring fluorescent emission.

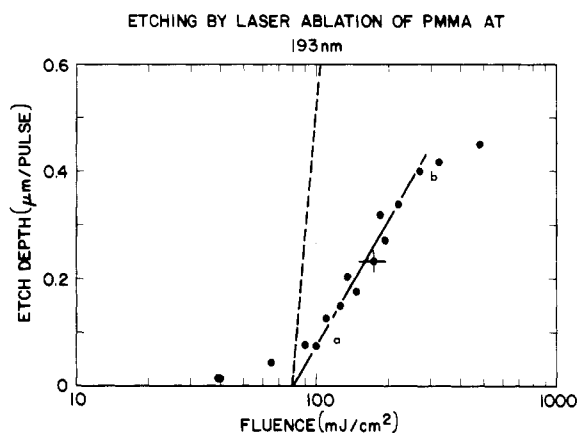


**Figure 3.** Plot of etch depth vs. fluence in the etching by laser ablation of PMMA ( $\bar{M}_n \sim 800\,000$ ) at 193 nm. The solid line is a least-squares fit of points that fall within the region of ablative photodecomposition. The dashed line is the line of shape  $1/\alpha$ , where  $\alpha$  is the absorptivity of PMMA at 193 nm from literature values.<sup>13</sup> The intercept for the dashed line was arbitrarily set to coincide with that for the solid line. The uncertainty in the experimental values is indicated in the data point at  $\sim 0.18$  J/cm<sup>2</sup>.

using the pure material to calibrate the GC-MS. For SEM studies, the PMMA samples were shadowed with gold and examined in a Hitachi scanning electron microscope. The geometry of the setup used for the laser-induced fluorescence (LIF) studies is shown in Figure 1. The electronic system that coupled the ablation pulse from the excimer laser to the fluorescence pump pulse from a dye laser and subsequently monitored the fluorescence signal is shown schematically in Figure 2. LIF studies were carried out only at 248 nm as the ablating wavelength. The UV pulses were repeated at 5 Hz. The polymer was translated slowly past the beam by a worm drive so that successive pulses struck a fresh surface.

## Results

**Products.** Three products of molecular weight greater than 30 were identified in the irradiation of PMMA with 193- or 248-nm laser radiation.<sup>10</sup> These were CO<sub>2</sub>, methyl methacrylate (MMA), and a solid whose infrared spectrum was identical with that of PMMA. The solid from 248-nm irradiation was available in sufficient quantity for molecular weight analysis. By gel permeation chromatography it was found to have  $\bar{M}_n = 2500$  and  $\bar{M}_w = 4500$ . It was readily soluble in carbon tetrachloride (solubility parameter,<sup>11</sup>  $\delta = 17.6$ ) and also in ethanol ( $\delta = 26.0$ ) at room temperature. A careful search was made for products such as methanol and methyl formate, which have been reported<sup>12</sup> to be formed in the photolysis at room temperature of PMMA with low intensity, continuous radiation at 254 nm, but no evidence was found for their presence among the products.

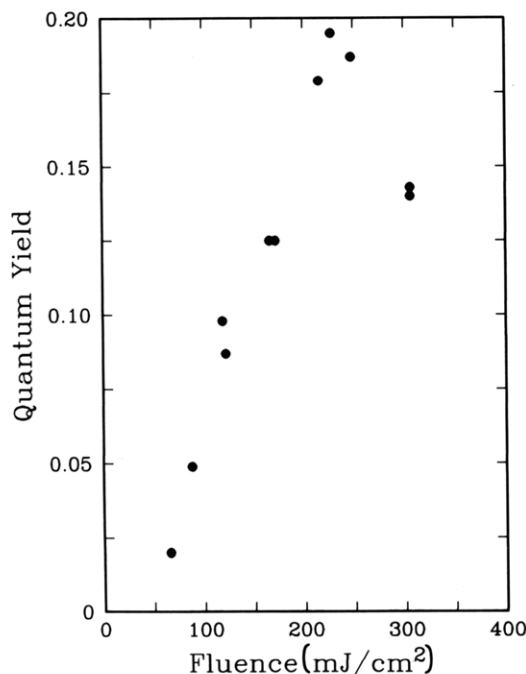


**Figure 4.** Quantum yields of monomer in laser ablation of PMMA ( $\bar{M}_n \sim 800\,000$ ) at 193 nm. Photons absorbed in the entire solid (not just in the ablated volume) are used in calculating the quantum yield. The absorption data for PMMA in the literature<sup>13</sup> were used.

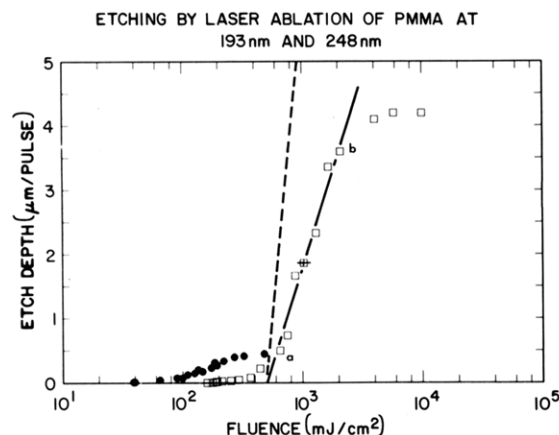


**Figure 5.** Plot of etch depth vs. fluence in the etching by laser ablation of PMMA ( $\bar{M}_n \sim 800\,000$ ) at 193 and 248 nm. Solid and dashed lines have the same significance as in Figure 3. Uncertainties are indicated in the data point at  $\sim 1\text{ J/cm}^2$ .

**Quantitative Studies.** In Figure 3 is plotted the etch depth per pulse as a function of fluence (on a logarithmic scale) for the etching of PMMA by 193-nm laser radiation. The quantum yields for the production of MMA in a series of parallel experiments are shown in Figure 4. The quantum yields were independent of the initial molecular weight of the polymer sample. Note that slow but measurable etching of the polymer occurred even below a fluence of  $65\text{ mJ/cm}^2$ , which is the point at which MMA is formed in detectable amounts. At a fluence of  $230\text{ mJ/cm}^2$ , the quantum yield of MMA reached a maximum value and decreased at greater fluence. The etch depth per pulse also started to level off above this value for the fluence. The principal error in these measurements is the fluctuation in the output of the laser from pulse to pulse. But for each point on the etch curve, the etch depth was determined by averaging the result of a number ( $>5$ ) of individual etchings. The uncertainty was  $\pm 8\%$  in the fluence and  $\pm 0.02\text{ }\mu\text{m}$  in etch depth.

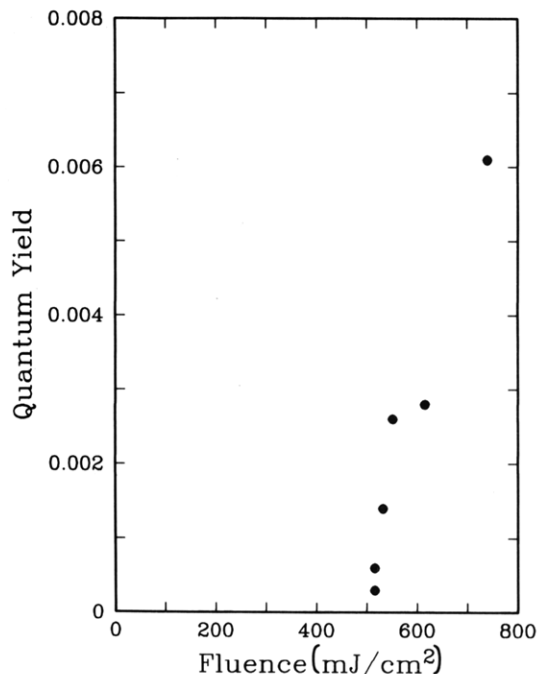


**Figure 6.** Quantum yields of monomer in laser ablation of PMMA ( $\bar{M}_n \sim 800\,000$ ) at 248 nm. Photons absorbed in the entire solid are used in the calculation of the quantum yield, using absorption data in the literature.<sup>13</sup>

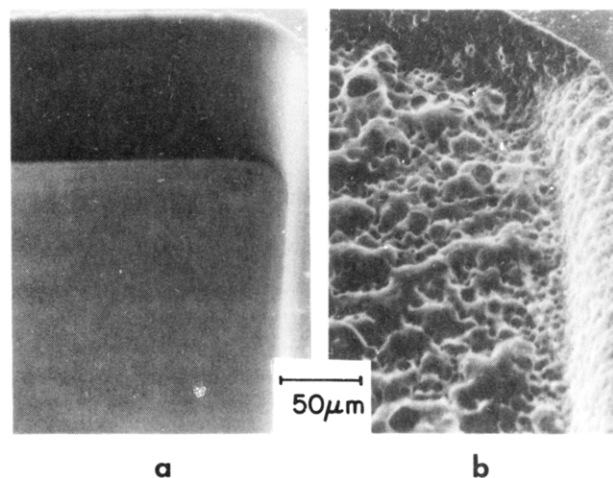


**Figure 7.** SEM photographs of the inside surface of etch pits produced by ultraviolet laser ablation of PMMA ( $\bar{M}_n \sim 800\,000$ ): (a) 193 nm, fluence of  $0.70\text{ J/cm}^2$ ; (b) 248 nm, fluence of  $2.70\text{ J/cm}^2$ .

In Figures 5 and 6 are plotted similar measurements on the exposure of PMMA to 248-nm laser radiation. The data at 193 nm are also shown here for comparison. The most important product of ablation at 248 nm was PMMA of low molecular weight. MMA was a minor product ( $<1\%$  chemical yield) compared to 193 nm (18% chemical yield).

SEMs of the etched surfaces of PMMA are shown in Figure 7. The textures of the surfaces obtained at the two wavelengths were not a function of the fluence. For the purpose of comparison, the fluences chosen here are at the high ends of the respective etch curves shown in Figures 3 and 5. SEM's of the solid material that is ejected from the polymer surface are shown in Figure 8. It is observed that the product at 248 nm has melted and coalesced into spheres whereas the sample at 193 nm does not show signs of being heated to its melting point.

Figure 9 shows the  $C_2$  band head signal from PMMA (ablating wavelength 248 nm) obtained by LIF detection

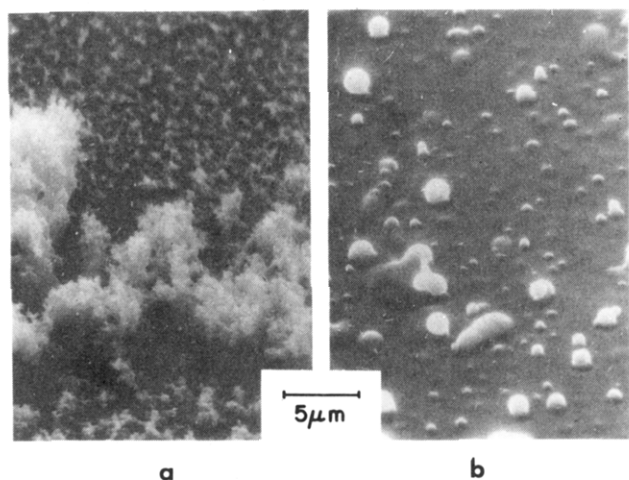


**Figure 8.** SEM photographs of solid material ejected during laser ablation of PMMA: (a) 193 nm, fluence of 0.15 J/cm<sup>2</sup>; (b) 248 nm, fluence of 2.70 J/cm<sup>2</sup>.

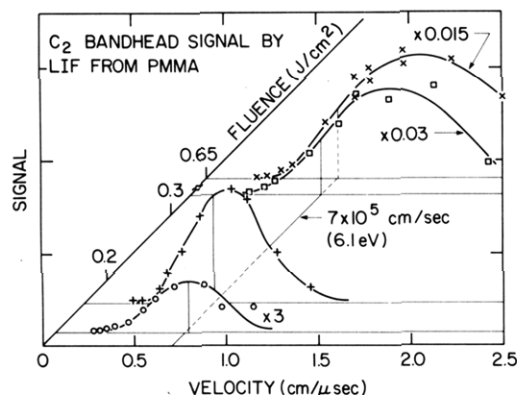


**Figure 9.** LIF signal from C<sub>2</sub> radicals indicating the distributions in velocities (as determined by time-of-flight). (UV radiation at 248 nm.) The solid curves are for the purpose of visualization.

of the ejected material. The pumping wavelength corresponded to 438.2 nm [(2,0) of the  $A^3\Pi_g \leftarrow x'^3\Pi_3$  transition] and the detection wavelength of 471.5 nm corresponded to (2,1) in the same transition. The velocities were calculated from the temporal delay between the UV pulse and the fluorescence excitation pulse since the ejected material was sampled at a known distance (1.65 cm) above the surface of the polymer (Figure 1). The uncertainty in the fluence of the ultraviolet laser was the principal error in these LIF measurements.

The LIF measurements also show a threshold fluence, above which the amplitude of the C<sub>2</sub> signal rises several hundredfold. Surprisingly, there is a small yield of C<sub>2</sub> at fluences as low as 0.12 J/cm<sup>2</sup>, which is significantly lower than the onset of material etching (0.65 J/cm<sup>2</sup>) at 248 nm. The maximum velocity of the C<sub>2</sub> doubled when the threshold fluence for ablation threshold is exceeded.

## Discussion

An examination of the etch depth vs. fluence curves in Figures 1 and 2 show three regions of differing slope. In earlier work on these and other polymers<sup>3b,4,9,13</sup> only the central region in which the etch depth increased rapidly with log fluence was noted and the conclusion was drawn<sup>3b,4,13</sup> that the etch depth per pulse was a linear function of log fluence in accordance with predictions based on Beer's Law. The present results on PMMA show that the onset of etching (the so-called "threshold fluence") is really not sharply defined. In the fluence region below

**Table I**  
**Laser Ablation Efficiencies of PMMA at 193 and 248 nm**

	PMMA			
	193 nm		248 nm	
absorptivity, cm <sup>-1</sup>	2.0 × 10 <sup>3</sup>	1.3 × 10 <sup>4</sup> <sup>a</sup>	5.7 × 10 <sup>2</sup>	1.6 × 10 <sup>3</sup> <sup>a</sup>
fluence, mJ	65 <sup>b</sup>	270 <sup>c</sup>	650 <sup>b</sup>	4060 <sup>c</sup>
etch depth/pulse, μm	0.04	0.40	0.50	4.1
mass ablated (mg)/joules absorbed (J)	3.77, 0.83 <sup>d</sup>	1.08, 0.25 <sup>d</sup>	1.48, 0.55 <sup>d</sup>	0.29, 0.15 <sup>d</sup>
quantum yield of monomer in ablated volume	23, 5.0 <sup>d</sup>	6.7, 1.6 <sup>d</sup>	7.1, 2.6 <sup>d</sup>	1.4, 0.8 <sup>d</sup>

<sup>a</sup> Value obtained from etch curve. <sup>b</sup> Onset of ablative photodecomposition. <sup>c</sup> Probable limit of ablative photodecomposition. <sup>d</sup> Value calculated with slope of etch curve.

"b" (Figures 3 and 5) the curves have a small slope and the only product to be detected in C<sub>2</sub>. The region between "b" and "a" can be called the region of ablative photodecomposition since absorption of the laser pulse results in (i) the expulsion of all of the material in a certain volume (the "ablated volume") as diatomic and triatomic species as well as monomer and low molecular weight polymer, (ii) the material expelled carries away most of the energy of the photon in excess of that which is needed for bond-breaking, and (iii) the material is expelled at supersonic velocities and the translational energy of the fragments accounts for a significant (~25%)<sup>6,14</sup> fraction of the incident photon energy. In order to understand the details of the bond-breaking process that precedes etching, it is necessary to evaluate the fraction of the incident energy that is absorbed in the ablated volume. Without explicit assumptions about the nature of the decomposition process, it can be derived (loc. cit) that

$$l_t = (1/\alpha) \log F/F_0 \quad (1)$$

where  $l_t$  is the etch depth at a fluence  $F$ ,  $\alpha$  is the absorptivity, and  $F_0$  is the threshold fluence. It follows that the slope of a plot of  $l_t$  vs.  $\log F$  should be  $1/\alpha$ . In Figures 3 and 5, a dashed line has the reciprocal of the absorptivity that would be predicted from a measurement of the ultraviolet absorption of a film of PMMA in a spectrometer.<sup>15</sup> There is obviously a serious disagreement between the slopes of the etch depth vs.  $\log F$  plots and the value of  $1/\alpha$  from UV spectrometry. Since etch depths are averaged over a number of successive pulses, the  $n$ th pulse sees a surface that has been altered in its UV absorption by the  $(n-1)$ th,  $(n-2)$ th, etc. pulses. However, in that case, the plot of etch depth vs. the number of pulses would not be linear in the initial region and the line from the later points would not pass through the origin. Since this is not the case,<sup>8</sup> the change in the absorption of the polymer seems to occur within a single pulse before ablation begins. It is therefore more reasonable to use the value of  $\alpha$  derived from Figures 3 and 5 rather than the values derived from UV absorption spectrometry. Table I summarizes the data in Figures 3 and 5, and the calculations based on these (last two rows) use both values of the absorption coefficient.

The onset of significant absorption (point "a" in Figure 3) at 193 nm (fluence 0.065 J/cm<sup>2</sup>) corresponds to 0.11 of the incident intensity being absorbed in the ablated volume while the limit (point "b") corresponds to a fraction of 0.70. If the quantum yields in Figure 4 are adjusted for the fraction of the radiation that is actually absorbed in the ablated volume, these range from 0.18 at "a" to 0.24 at "b".

These values are essentially the same within the experimental uncertainty. The drop off in the etch curve that coincides with the drop in the yield of MMA suggests that at fluences greater than  $0.23 \text{ J/cm}^2$  the absorption of the tail end of the laser pulse by the MMA that is being ejected from the surface serves to limit the etching and also destroys some of the MMA by secondary photolysis.

At 248 nm, the region of significant etching extends from fluences of  $0.65 \text{ J/cm}^2$  (point "a") to  $4.06 \text{ J/cm}^2$  (point "b"). The corresponding fractions of the incident radiation that are absorbed in the ablated volume are 0.17 and 0.78, respectively. The quantum yields in Figure 6 not only are over a smaller range of fluence but also suffer from a large uncertainty because of the difficulty in collecting and analyzing the small yield of MMA. The values of the corrected quantum yields over the fluence range in Figure 6 is 0.002–0.008. Clearly, the chemistry of the formation of MMA at the two wavelengths is quite different.

Since the major portion of the PMMA that is ejected from the surface is in the form of a solid polymer, it is of interest to compare the efficiency of this process in terms of both photons and energy at the two wavelengths. These values are given in Table I. The last two rows in this table represent the same data. If the mass of the expelled material is related to the energy that is needed to ablate it, the values at 193 and 248 nm are remarkably overlapping. If the same numbers are expressed in terms of the number of monomeric units (not necessarily monomers) per quantum of light, there is still some overlap but the process at 193 nm is seen to be much more efficient than the process at 248 nm.

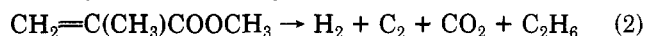
Two mechanisms have been considered for the UV laser ablation of polymers. The first proposes<sup>3b,4,16</sup> that there is initial excitation to an electronic level but these upper states internally convert to "hot" ground states. Subsequent decomposition is therefore a pyrolysis of the polymer that is not very different from the processes that are observed with laser radiation at visible or infrared wavelengths. The second mechanism<sup>2,9,13</sup> proposes that ablation proceeds from photochemical decomposition of the initially formed electronically excited states.

The thermal mechanism can be analyzed readily in the case of PMMA from the data in Table I. Since the specific heat of PMMA is  $0.35 \text{ cal/(deg}\cdot\text{g)}$ , the average value for the mass ablated per joules absorbed at 193 nm, which is 0.53 can be used to calculate that the temperature in the ablated volume will rise by 1260 K. The thermal degradation of PMMA to give MMA has been studied in detail by Jellinek and Luh.<sup>17</sup> Two kinds of initiation processes govern the reaction. Of these, if one picks the chain-end-initiated reaction since it is considerably faster than the random-initiated reaction, the Arrhenius parameters for a sample of  $\bar{M}_n = 960\,000$  are  $A = 2.89 \times 10^8 \text{ min}^{-1}$  and  $E = 25300 \text{ cal/mol}$ . This leads to a half-life for decomposition at a temperature of 1533 K ( $1260 + 273$ ) of 0.4 ms. Since the laser pulse lasts for only 15–25 ns (FWHM) and the products arrive at the sampling zone for LIF measurement, which is 16 mm away, in the order of  $1 \mu\text{s}$  after the laser pulse, the thermal degradation rate is too slow by several orders of magnitude to account for the ablation process.<sup>18,19</sup>

The photochemical mechanism would account for many of the observed features of the ultraviolet laser ablation process, such as the variation in the chemistry of the products between 193 and 248 nm. It is probable that there is a considerable difference in the quantum yield for the primary bond-breaking between the two wavelengths. It is known that in the far-UV, even in the condensed

phase, photochemical transformations in small organic molecules proceed with quantum yields that approach unity.<sup>20</sup> At 248 nm, the quantum yield would be expected to be an order of magnitude smaller but it can increase if there is a local rise in temperature so that thermally activated photoprocesses become possible. The molten condition of the expelled solid material that is evident in Figure 8 shows that this explanation is plausible.

In addition to the one-photon process discussed above, the LIF data show that simultaneously there is also a multiphoton decomposition of PMMA that is taking place. The decomposition of MMA to yield  $\text{C}_2$  may proceed according to the following stoichiometry:



This does not imply that such a chemical reaction actually occurs. It is shown merely to demonstrate one low-energy path to  $\text{C}_2$ . From standard heats of formation, it can be shown that to produce a  $\text{C}_2$  molecule with 6 eV of translational energy a minimum of 3 photons of 248-nm wavelength ( $=5 \text{ eV}$ ) will be needed. It is surprising that even below the threshold for ablation of  $0.65 \text{ J/cm}^2$ , at which point there is on average 1 photon per 2.6 monomer units in the ablated volume of the polymer,  $\text{C}_2$  can be detected with this supersonic velocity. There must be a multiphoton process to give  $\text{C}_2$  that proceeds in parallel with the one-photon process that causes single bond breaks in the polymer chain.

Woodward, Chupka, and Colson have proposed<sup>21</sup> a cyclic pumping mechanism to account for the multiphoton decomposition that results in  $\text{C}_2$  being formed from small molecules during high-power UV laser (picosecond) pulse irradiation. Since the laser pulses used in the present study were more than 10 ns long and the absorption by the PMMA itself is weak, the multiphoton decomposition must be ascribed to a few absorption centers within the polymer where there is a local concentration of the radiation ("speckle") or there are impurities present that can lead to more intense absorption and an explosive decomposition. Such a mechanism can be duplicated by introducing 1 or 2% of a strong absorber in the PMMA to see its effect on the ablation behavior.<sup>22</sup>

A more important role for the multiphoton process may also be operative. Ablative photodecomposition is viewed principally as a volume explosion<sup>23</sup> in which the volume change of 30% in going from PMMA to MMA is seen to be augmented by the energy of the photon that is in excess of the bond-dissociation energy. At 193 nm, where 18% of the polymer is decomposed to the monomer, the resulting volume change may be adequate to cause ablation. But at 248 nm where there is very little monomer produced and the polymer is decomposed to oligomers consisting of 25–40 or more monomeric units, the propulsive force for the ablation is less evident. The multiphoton decomposition may serve just such a purpose. The decomposition of a few monomer units to several small fragments (including  $\text{C}_2$ ) will act as an explosive charge to ablate the polymeric fragments out of the ablated volume with considerable velocity. Tests to verify this hypothesis are being undertaken.

An attempt to fit the velocity distribution of the  $\text{C}_2$  molecules to a Maxwell-Boltzmann distribution is shown in Figure 10. Even at the fluence that was picked, which was well below the threshold for ablation, the fit is less than perfect. This can be attributed to the nonthermalization of the source of the  $\text{C}_2$  species and is reminiscent of the initial transition into a supersonic (adiabatic) expansion.<sup>24</sup> In contrast, the data of Viswanathan and Hussla<sup>25</sup> on the velocity distribution of Cu atoms and  $\text{Cu}^+$

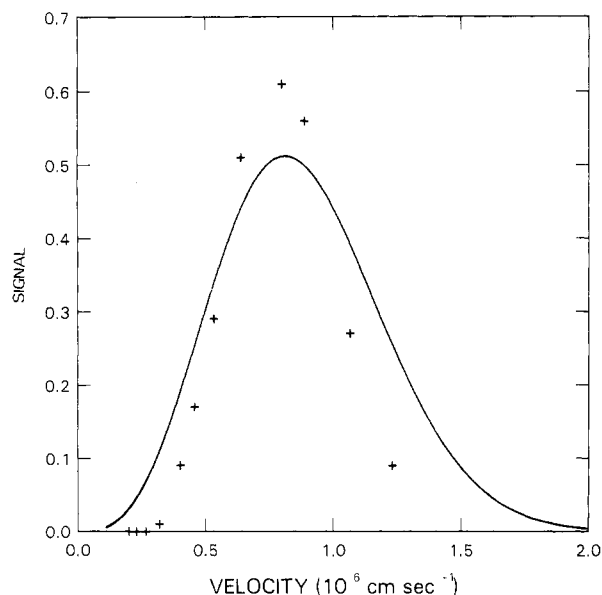


**Figure 10.** LIF signal from  $C_2$  radicals as a function of their velocity. The solid line represents the free expansion of a Boltzmann Distribution. Fluence of  $0.16 \text{ J/cm}^2$  at  $248 \text{ nm}$ .

ions from the laser ablation of a copper crystal at the same wavelength and pulse width as used here fits a Maxwell-Boltzmann distribution quite well. In this instance, there can be no doubt that the laser energy heats and vaporizes the atoms of copper. The translational temperature of the neutral copper atoms was  $22\,000\text{--}27\,000 \text{ K}$ , whereas the temperature of the  $C_2$  atoms in the present case was  $40\,000 \text{ K}$ .

The technological interest in UV laser ablation of polymers stems to a considerable degree from the lack of thermal damage to the material that surrounds the etched surface<sup>1,3,4</sup>. Although complex explanations are possible to account for this observation,<sup>26</sup> it may also result from the limited rise ( $<200 \text{ K}$ ) in temperature in the ablated volume, a situation that is possible in a purely photochemical process. In this sense, ablative photodecomposition is a novel method of cleaving a polymeric organic solid since it occurs in an electronically excited state of the concerned bonds. Its relevance to the cutting of live tissue has been pointed out elsewhere.<sup>27</sup>

**Acknowledgment.** We thank Drs. K. Eissenthal of Columbia University, L. Hadel of Rutgers University, and B. J. Garrison of Pennsylvania State University for many stimulating discussions. We express our indebtedness to Professor D. von der Linde and B. Danielzik of the University of Essen and Professor P. Dyer of the University of Hull for making their data available prior to publication.

**Registry No.** PMMA (homopolymer), 9011-14-7.

## References and Notes

- (1) Srinivasan, R.; Mayne-Banton, V. *Appl. Phys. Lett.* **1982**, *41*, 576.
- (2) Srinivasan, R.; Leigh, W. J. *J. Am. Chem. Soc.* **1982**, *104*, 6784.
- (3) (a) Geis, M. W.; Randall, J. N.; Deutsch, T. F.; DeGraff, P. D.; Krohn, K. E.; Stern, L. A. *Appl. Phys. Lett.* **1983**, *43*, 74. (b) Deutsch, T. F.; Geis, M. W. *J. Appl. Phys.* **1983**, *54*, 7201.
- (4) Andrew, J. E.; Dyer, P. E.; Forster, D.; Key, P. H. *Appl. Phys. Lett.* **1983**, *43*, 717.
- (5) Murahara, M.; Kawamura, Y.; Toyoda, K.; Namba, S. *Oyo Butsuri* **1983**, *52*, 83.
- (6) Davis, G. M.; Gower, M. C.; Fotakis, C.; Efthimiopoulos, T.; Argyrakos, P. *Appl. Phys. A* **1985**, *A36*, 27.
- (7) Srinivasan, R.; Dreyfus, R. W. In "Laser Spectroscopy"; Hansch, T. W.; Shen, Y. R., Eds.; Springer-Verlag: New York, 1985; Vol. 7, p 396.
- (8) Srinivasan, R. *J. Radiat. Curing* **1983**, *4*, 12.
- (9) Srinivasan, R.; Braren, B. *J. Polym. Sci., Polym. Chem. Ed.* **1984**, *22*, 2601.
- (10) Analysis of the gaseous products from the ablation of PMMA by  $193\text{-nm}$  laser pulses by time-of-flight mass spectrometry has recently been reported. (Danielzik, B.; Fabricus, N.; Rowekamp, M.; von der Linde, D. *Appl. Phys. Lett.* **1986**, *48*, 212.)
- (11) Brydson, J. A. "Plastics Materials"; Butterworth Scientific: Boston, 1982; p 76.
- (12) Gupta, A.; Liang, R.; Tsay, F. D.; Moacanin, J. *Macromolecules* **1980**, *13*, 1696.
- (13) Jellinek, H. H. G.; Srinivasan, R. *J. Phys. Chem.* **1984**, *88*, 3048.
- (14) Srinivasan, R.; Liu, S.-H.; Dreyfus, R. W. unpublished work.
- (15) Lin, B. J. *J. Vac. Sci. Technol.* **1975**, *12*, 1317.
- (16) Koren, G.; Yeh, J. T. C. *Appl. Phys. Lett.* **1984**, *44*, 1112.
- (17) (a) Jellinek, H. H. G.; Luh, M. D. *J. Phys. Chem.* **1966**, *70*, 3672. (b) Jellinek, H. H. G.; Luh, M. D. *Makromol. Chem.* **1968**, *115*, 89.
- (18) Time-resolved measurement of the acoustic wave that is transmitted through the polymer film during ablation of polyimide films at  $193 \text{ nm}$  shows that the delay between the UV pulse and the acoustic wave is of the order of  $4 \text{ ns}$ . (Dyer, P., private communication).
- (19) Garrison and Srinivasan (*J. Appl. Phys.* **1985**, *52*, 2909) have modeled the ablation of a PMMA-like polymer based on a photochemical as well as a photothermal process. Within the limits of their assumptions, the photothermal process requires fourfold greater energy to ablate unit mass of material than the photochemical model.
- (20) von Sonntag, C.; Schuchmann, H.-P. *Adv. Photochem.* **1977**, *10*, 59.
- (21) Woodward, A. M.; Chupka, W. A.; Colson, S. D. *J. Phys. Chem.* **1984**, *88*, 4567. See also: Chen, P.; Pallix, J. B.; Chupka, W. A.; Colson, S. D. *Chem. Phys. Lett.*, to be published.
- (22) The introduction of  $0.4 \text{ mol } \%$  of acridine in PMMA lowers the threshold for ablation at  $248 \text{ nm}$  from  $0.65$  to  $0.35 \text{ J/cm}^2$  (Hadel, L.; Braren, B.; Srinivasan, R. to be published).
- (23) Garrison, B. J.; Srinivasan, R. *Appl. Phys. Lett.* **1984**, *44*, 849.
- (24) Lou, Y. S. *J. Appl. Phys.* **1971**, *42*, 536. Gordon, R. J.; Lee, Y. T.; Herschbach, D. R. *J. Chem. Phys.* **1971**, *54*, 293. Anderson, J. B.; Fenn, J. B. *Phys. Fluids* **1965**, *8*, 780. Saenger, K. L.; Fenn, J. B. *J. Chem. Phys.* **1983**, *79*, 6043.
- (25) Viswanathan, R.; Hussla, I. In "Laser Processing and Diagnostics"; Bauerle, D., Ed.; Springer: New York, 1984 Springer Series in Chemical Physics, *39*, 148.
- (26) Melcher, R. L. In "Laser Processing and Diagnostics"; Bauerle, D., Ed.; Springer: New York, 1984; Springer Series in Chemical Physics, *39*, 418.
- (27) Moretti, M. *Lasers Appl.* **1985**, *50*.